Dielectrowetting on curved surfaces

Applied Physics Letters

Dielectrowetting on curved surfaces

Cite as: Appl. Phys. Lett. **120**, 191601 (2022); https://doi.org/10.1063/5.0092216
Submitted: 22 March 2022 • Accepted: 29 April 2022 • Published Online: 10 May 2022

É. Ruiz-Gutiérrez, P. J. Baker, A. M. J. Edwards, et al.

AIP Publishing

Applied Physics Letters ARTICLE scitation.org/journal/apl

Dielectrowetting on curved surfaces

Cite as: Appl. Phys. Lett. **120**, 191601 (2022); doi: 10.1063/5.0092216
Submitted: 22 March 2022 · Accepted: 29 April 2022 ·
Published Online: 10 May 2022

É. Ruiz-Gutiérrez,[1,2] P. J. Baker,[3] A. M. J. Edwards,[3,4] M. I. Newton,[3] I. C. Sage,[3] R. Ledesma-Aguilar,[1] G. McHale,[1] and C. V. Brown[3,a)]

AFFILIATIONS

[1]Institute for Multiscale Thermofluids, School of Engineering, The University of Edinburgh, Robert Stevenson Road, Edinburgh EH9 3FB, United Kingdom
[2]School of Engineering, Newcastle University, Stephenson Building, Newcastle upon Tyne NE1 7RU, United Kingdom
[3]SOFT Group, School of Science and Technology, Nottingham Trent University, Clifton Lane, Nottingham NG11 8NS, United Kingdom
[4]Department of Physics, Loughborough University, Loughborough LE11 3TU, United Kingdom

[a)]Author to whom correspondence should be addressed: carl.brown@ntu.ac.uk

ABSTRACT

Programmable fluidic systems on curved and flexible substrates are of increasing interest. One approach to achieving programmability is the controlled sequential wetting and dewetting on a surface using voltage actuation. In particular, liquid dielectrophoresis techniques have recently been shown to provide the ability to form a spread liquid film on a normally liquid repellent, but rigid, substrate via applying a spatially periodic electrical potential underneath an initial sessile droplet. In this work, we demonstrate the creation of thin, rectangular shaped, films of electrically insulating liquid on the side of a curved and flexible liquid repellant substrate using dielectrophoresis forces. We find that the experimental threshold voltage $V_T(\kappa_s)$ for film formation has a monotonic dependence on the value of the substrate curvature κ_s in the range $-0.4\,\mathrm{mm}^{-1} < \kappa_s < 0.26\,\mathrm{mm}^{-1}$. By considering the balance of stresses acting on the films, including the Laplace pressure and the Maxwell stress, we develop an analytical theoretical expression that is in excellent quantitative agreement with our curvature dependent experimental threshold voltage measurements. The resulting physical insights and the demonstration of programmable wettability on curved and flexible substrates with both positive and negative curvature provide the foundations for applications in imaging, displays, and biochemical analysis.

The electrical manipulation and actuation of small quantities of liquids, using either electrowetting or dielectrophoresis, have been established as important tools in applications such as optofluidics and biomicrofluidics.[1–4] In flat rigid enclosed geometries that contain two immiscible liquids, voltage control over the shape of the interface between liquids with different refractive indices has been used to create focus-tunable liquid lenses, while for biochemical analysis applications, selective actuation of one of the liquids has been achieved using voltage addressable substrate electrodes to move the three-phase contact line.[5,6] In flat rigid open-to-air geometries, *in situ* voltage forced wetting of a single liquid droplet onto a liquid repellent surface, droplet dispensing, and droplet transport actuated by controlled wetting and dewetting on a surface via sequential voltage activation of adjacent electrodes have been extensively explored.[7,8]

A few studies have investigated how electrically controlled fluidic systems can be created in non-flat architectures, with curved and/or flexible substrates. Examples of enclosed systems include both electrowetting and dielectrophoresis based liquid lenses encapsulated by flexible curved substrates that provide an expanded field of view and reconfigurability,[9–12] and the demonstration of digital droplet microfluidics within a flexible curved wrist band.[13] Examples of open systems include the actuation of droplets in air on a flexible substrate for temperature sensing applications[14] and the demonstration of electrowetting on a dielectric with curved paper-based substrates for environmentally sustainable display applications[15] and on the surface of a sphere for studying wetting morphologies and droplet detachment.[16–18]

Liquid dielectrophoresis has been recently shown to permit the voltage induced complete spreading of a liquid onto a normally liquid repellent open surface. This phenomenon permits the formation of a fine liquid filament when a voltage is applied between coplanar electrodes on the solid surface, and the filament can be programmed to breakup into a pre-defined array of dispensed droplets.[19–21] While in dielectrowetting, a voltage applied between interdigitated fingers of a two-dimensional array of coplanar electrodes creates a spread liquid

film that can be dewetted back into the original sessile droplet state on demand.[22,23] Spreading across adjacent inter-locking electrode regions with sequentially applied and removed voltages enables transport of discrete droplets, known as digital droplet microfluidics.[24] The production of liquid filaments or spread liquid films is not possible using electrowetting, for which contact angle saturation limits the extent of voltage forced wetting of a droplet.[25] The interface localized liquid dielectrophoresis effect originates when dielectrophoresis forces act on the dipoles in a liquid that are polarized by the non-uniform electric fields created between the patterned electrodes on the surface underneath the liquid.[26,27] In this work, we demonstrate and analyze dielectrowetting on a non-flat curved surface formed by having a non-rigid, i.e., flexible, substrate. We first describe how we have produced full voltage induced spreading of an electrically insulating liquid to form a thin liquid film on the side of a curved, liquid repellent, flexible plastic substrate that has a bendable interdigital transparent electrode pattern on its surface.

Figure 1 shows the device architecture and the experimental geometry. The flexible device substrate was a 0.2 mm thick polyethylene terephthalate (PET) foil covered by a transparent conducting indium tin oxide layer (ITO) of resistivity 100 Ω/sq (Product 749737, Sigma Aldrich, Darmstadt, Germany). The indium tin oxide was etched using photolithography into an interdigitated coplanar electrode pattern covering an area of length $l = 10$ mm and width $w = 2$ mm, as shown in Fig. 1(b). Both the electrode linewidths and the size of the gap between adjacent electrodes equaled $d = 60\ \mu$m. The surface of the device was capped with a protective 1 μm insulating layer of SU8-2 photoresist (Micro Resist Technology GmbH, Berlin, Germany) and over-coated with a thin, <100 nm, liquid repellent surface layer of Teflon AF (CAS 37626-13-4, Sigma-Aldrich/Merck KGaA, Darmstadt, Germany). All experiments were performed in a temperature-controlled laboratory (21 ± 1 °C).

Our flexible device substrate was clamped by its edges and initially held as a flat rectangular surface, vertically oriented in the x–z plane with its short edge aligned in the vertical z-direction, as shown in Figs. 1(a) and 1(b). A droplet of the electrically insulating liquid TMP-TG-E (trimethylolpropane triglycidyl ether, CAS Number 3454-29-3, Sigma Aldrich, Darmstadt, Germany) was dispensed onto the center of the electrode area using a Gilsen pipette. TMP-TG-E has a high dielectric constant of $\varepsilon_L = 13.8$, a surface tension of $\gamma = 0.043 \pm 0.001$ N m^{-1}, and a mass density of $\rho_L = 1157 \pm 10$ kg m^{-3}. The TMP-TG-E formed a sessile droplet on the liquid repellent substrate with a base diameter of 3.00 ± 0.05 mm, static contact angle of $\theta_S = 72° \pm 2°$, and volume of $\Omega = (7.5 \pm 0.8) \times 10^{-9}$ m^3. The droplet remained attached in place on the side of vertical substrate surface since its contact angle was less than 90°, although its diameter was above the capillary length for the liquid, $L_c = \{\gamma/[(\rho_L - \rho_{air})g]\}^{1/2} \approx 1.9$ mm.

Applying an AC sinewave voltage with RMS amplitude V_b and a frequency of 500 Hz to each alternate electrode, Fig. 1(b), produced highly non-uniform electric fields that decayed into the liquid immediately above the electrodes. For voltages where $V_b > 100$ V (RMS), the resultant surface localized dielectrophoresis forces flattened and elongated the droplet, increasing its base width in the x-direction parallel to the electrode stripes.[4,23,26,27] There was a commensurate decrease in the droplet thickness h and the droplet contact angle, $\theta(V_b) < \theta_S$. Applying a voltage in the range $358\ \text{V} < V_b < 370$ V resulted in full spreading to form a liquid film state that covered the 10×2 mm^2 electrode area on the side of the vertically oriented surface, shown from the side and from the top in Figs. 2(c) and 2(d), respectively. On a flat surface, the liquid droplet spreads to form a film when the applied voltage exceeds a threshold value V_T that would cause the voltage dependent $\theta(V_b)$ contact angle to go to zero. According to the dielectrowetting extrapolation formula for a flat non-curved surface, this full spreading occurs when $\cos[\theta(V_b = V_T)] = \cos[\theta_S] + \beta V_b^2 = 1$, where β is the dielectrowetting coefficient.[23]

We then demonstrated the formation of spread liquid films on concave and convex curved substrates. We produced a curvature of radius R of the center of the curved flexible substrate by adjusting the distance between the gripping clamps, where we define the curvature as $\kappa_s = -1/R$. Figure 2 shows photographs of spread liquid films for three curvatures, for the liquid on the inside of a concave surface with $\kappa_s = -0.40$ mm^{-1} and $V_b = V_T = 380$ V in (a) and (b), for the liquid on the side of a flat surface with $\kappa_s = 0$ mm^{-1} and $V_T = 369$ V in (c) and (d), and for the liquid on the outside of a convex surface with $\kappa_s = 0.26$ mm^{-1} and $V_T = 362$ V in (d) and (e). In Fig. 2, side on views from along the y-direction are shown in the left-hand column and top views from along the z-direction are shown in the right-hand column. An ink dot visible on the substrate aided initial placement of the liquid drop onto the transparent electrode area [removed from Fig. 2(c) for clarity].

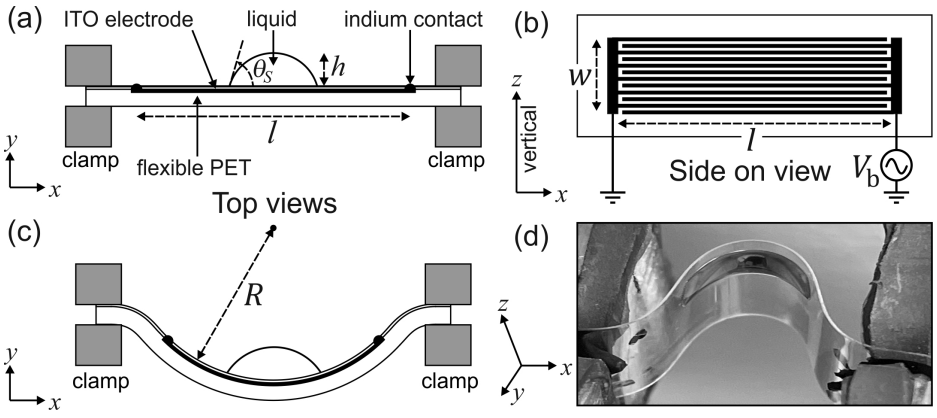

FIG. 1. Schematic diagrams of the device and the experimental geometry: (a) top view and (b) side on view. (a) The clamped rectangular flexible PET substrate, which was coated with transparent conducting indium tin oxide. (b) The interdigitated electrode array pattern etched into the ITO layer. (c) Moving the gripping clamps closer together caused the substrate to form a curve with central radius of curvature R. (d) Photograph of the curved substrate with a droplet of the liquid TMP-TG-E spread on the electrodes when $V_b = 369$ V.

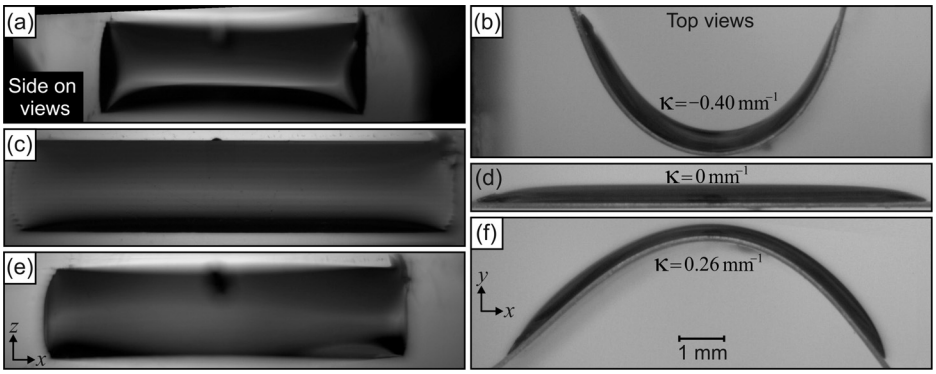

FIG. 2. Photographs of a spread film of the liquid TMP-TG-E on the flexible PET substrate as it was being held at three different curvature values κ_s, where $\kappa_s = -1/R$. Images (a) and (b) show a top view and a side-on view, respectively, of the liquid film on a substrate with curvature $\kappa_s = -0.40\,\mathrm{mm}^{-1}$ and film formation voltage $V_T = 380\,\mathrm{V}$. In images (c) and (d) $\kappa = 0\,\mathrm{mm}^{-1}$ and $V_T = 369\,\mathrm{V}$, and in images (e) and (f) $\kappa_s = 0.26\,\mathrm{mm}^{-1}$ and $V_T = 362\,\mathrm{V}$.

For each different curvature value, we initially abruptly applied a voltage of $V_b = 350\,\mathrm{V}$, and then we gradually increased the voltage amplitude quasi-statically in 1 V steps until the point at which the advancing edges of the film reached both the right and left edges of the electrode area. We defined the liquid film formation voltage V_T as the value of the applied voltage V_b, for which the length of arc of the base of liquid film just became exactly equal to the electrode length, $l = 10\,\mathrm{mm}$, at the film's center and widest point in the vertical direction. By performing our study with the liquid on the side of the vertically oriented substrate, we demonstrate that voltage forced film formation can be achieved for any substrate orientation while avoiding gravitational pooling of the liquid in the center of the spread film when $\kappa_s < 0$ or pooling at the edges of the spread film when $\kappa_s > 0$.

We have, hence, measured the quantitative effect that the curvature of the substrate has on the magnitude of the voltage $V_T(\kappa_s)$ at which the liquid film state is formed, for a range of curvature values κ_s. We find a systematic dependence of the liquid film state formation voltage on the curvature, with $V_T(\kappa_s)$, on average, reducing by 0.7% (2.5 V) per $0.1\,\mathrm{mm}^{-1}$ increase in the curvature κ_s. It would be very challenging to accurately quantify changes of this magnitude using other measurements, such as the curvature and voltage dependent contact angle $\theta(V_b)$ or length of arc of the base of the film. These latter quantities have inherent experimental uncertainties and are insufficiently reproducible due to changes in droplet position and pinning forces. Our meticulous while facile procedure of gradually increasing the voltage until the spread film base length equals the electrode width l overcomes these challenges because the edge of the fixed electrode pattern precisely defines an equal film base length for each measurement performed at different curvature values.

Figure 3 shows our experimental results of the voltage difference $\Delta V_T(\kappa_s)$ between the liquid film formation voltage on a curved substrate surface $V_T(\kappa_s)$ and liquid film formation voltage on a flat surface $V_T(\kappa_s = 0)$ as a function of κ_s. Experimental measurements were performed starting from the negative curvatures and progressing to the positive curvatures. Two experimental datasets shown in Fig. 3 by the open diamonds and the open circles symbols were taken using the same droplet and substrate. The liquid film formation voltage was measured for a flat substrate between each of the measurements of $V_b(\kappa_s)$ on a curved substrate, where the $V_b(\kappa_s = 0)$ value was an average of the values immediately before and after each measurement of $V_b(\kappa_s)$. This procedure compensated for the changes in the ITO resistivity due to bending, which were pronounced at large, particularly positive, curvatures. From an auxiliary measurement of the resistance of an unetched ITO coated PET strip of dimension $25 \times 7\,\mathrm{mm}^2$, the flat substrate resistance of $0.5\,\mathrm{k\Omega}$ when $\kappa_s = 0\,\mathrm{mm}^{-1}$ increased under curvature to $1.7\,\mathrm{k\Omega}$ when $\kappa_s = -0.4\,\mathrm{mm}^{-1}$, and to $100\,\mathrm{k\Omega}$ when $\kappa_s = 0.4\,\mathrm{mm}^{-1}$. We found that $V_T(\kappa_s = 0)$ varied in the range 358 ± 1 to $368 \pm 1\,\mathrm{V}$ for experiment 1, and in the range 362 ± 1 to $370 \pm 1\,\mathrm{V}$ for experiment 2. Measurements were repeated three times, for both $V_T(\kappa_s)$ and for $V_T(\kappa_s = 0)$, and the resulting average was used in each case. The vertical error bars on $\Delta V_T(\kappa_s)$ in Fig. 3 reflect the statistical variations in both of these quantities.

We now develop a two-dimensional theory to describe the spreading of the droplet into a film that has been formed by the action of the voltage V_b. We solve the balance of stresses in the direction normal to the liquid–gas interface to find the shape of the film, these are the capillary force, the Maxwell stresses, $\langle f_{el} \rangle$,[28] and the pressure jump, Δp, across the liquid–air free surface,

$$-\gamma M - \langle f_{el} \rangle + \Delta p = 0, \tag{1}$$

where M is the local curvature of the interface.[29]

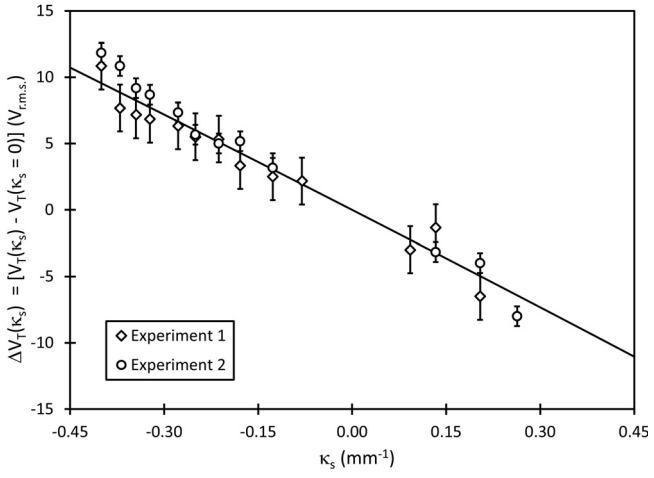

FIG. 3. The difference, $\Delta V_T(\kappa_s)$, between the liquid film formation voltage on a curved substrate surface $V_T(\kappa_s)$ and liquid film formation voltage on a flat surface $V_T(\kappa_s = 0)$, plotted against the value of the substrate curvature, κ_s. Data from two separate sets of measurements are shown by the open diamonds (experiment 1) and the open circles (experiment 2). The solid line is a plot of Eq. (5), without using fitting parameters.

For the second term in Eq. (1), it can be shown that

$$\langle f_{el} \rangle = -\frac{\pi\gamma}{d} E_l e^{-\pi\zeta/d}\left(1 - \frac{d\kappa_s}{\pi}\right) \tag{2}$$

(see the supplementary material for the full derivation), where ζ is the distance from the substrate, $E_l = \Phi\,\varepsilon_o(\varepsilon_L - \varepsilon_{air})V_b^2/2\gamma d$ is a dimensionless number that measures the intensity of the electric forces in relation to surface tension,[30] Φ is a constant found to be $\Phi \approx 0.23$ according to our mathematical model, and the other symbols were defined earlier.

We express the curvature of the liquid–gas interface as $M = -\sin\phi\,\mathrm{d}\phi/\mathrm{d}\zeta$, where ϕ is the local angle of the interface with respect to the solid substrate. Therefore, we can express Eq. (1) as an ordinary differential equation for ϕ. To integrate this differential equation, we set the boundary conditions, namely, the contact angles $\phi = \theta_S$ at $\zeta = 0$ and $\phi = 0$ at $\zeta = h$, implying that the interface becomes parallel to the substrate at its nominal thickness h. This results in

$$1 - \cos\theta_S = E_l(1 - e^{-\pi h/d})\left(1 - \frac{d\kappa_s}{\pi}\right) + \frac{h\,\Delta p}{\gamma} = 0. \tag{3}$$

Equation (3) has two unknowns, namely, E_l and Δp, therefore, to solve the system; we require one more equation. We invoke Eq. (1) once again and assume that for the liquid film to cover conformally the substrate, the interface assumes the curvature of the substrate, $M \approx \kappa_s$. The balance of forces implies

$$-\kappa_s + \frac{\pi}{d} E_l e^{-\pi h/d}\left(1 - \frac{d\kappa_s}{\pi}\right) + \frac{\Delta p}{\gamma} = 0 \tag{4}$$

and, together with Eq. (3), we can express the electric potential as a function of the film thickness.

We now express the film thickness in terms of the spreading length of the film. We assume that, at $V_b = V_T$, the cross-sectional area of the film $A = \Omega/w$ is a constant for the whole arc length l of the film, and make the approximation of a cylindrical film of constant thickness h, i.e., $h = \Omega/Lw - \kappa(\Omega/Lw)^2/2$. After substitution and some algebraic manipulation, we arrive at

$$\Phi\frac{\Delta\varepsilon V_T^2}{2\gamma d} = \frac{1-\cos\theta_S}{1-(1+q)e^{-q}} + \frac{1-q-\cos\theta_S+e^{-q}\left(q^2+q^3/2+\left(1+q-q^3/2\right)\cos\theta_S\right)}{4\pi\left(1-(1+q)e^{-q}\right)^2}d\kappa_s, \tag{5}$$

where $q = \pi\Omega/lwd$.

We note that a first order expansion of Eq. (5) could be produced, using the approximation that $V_T^2(\kappa_s) - V_T^2(\kappa_s = 0) \approx 2\Delta V_T V_T^{ave}$, that is linear in the curvature, κ_s. We evaluate the full Eq. (5) by substituting in the values for the parameters Ω, d, w, l, θ_S, γ, and ε_L, given above and plotted as the solid line on the graph of $\Delta V_T(\kappa_s)$ vs κ_s in Fig. 3. The prediction of Eq. (5) is in excellent agreement with the experimental results, especially given that there are no free fitting parameters in our theory. The liquid film formation voltage at zero curvature predicted by Eq. (5), $V_T(\kappa_s = 0) = 372.9\,\mathrm{V}$, is slightly higher than the experimental values, in part due to the analytical value for Φ obtained by discarding higher order terms.

Both our experiments and the theoretical model, Fig. 3, show an increase in the liquid film formation voltage, V_T, for negative curvature, $\Delta V_T(\kappa_s < 0) > 0$, and a decrease in the liquid film formation voltage for a positive curvature, $\Delta V_T(\kappa_s > 0) < 0$, when compared to the flat surface case. This can be explained as the combined effect of the change in the electric field due to the curvature of the electrodes and changes in the pressure. As it has been shown in Eq. (2), the electric forces decrease with the curvature of a concave surface. This is expected as electrodes in a closed loop cancel the electric field as the center of the loop is approached. On the other hand, for a droplet in static equilibrium and finite contact angle, $0 < \theta(V_b) < \theta_S$, the Laplace pressure is proportional to the curvature of the liquid surface. This is because the electric stresses remain close to the contact line, and we are neglecting gravitational effects. However, as the droplet is flattened, $\theta(V_b) \to 0$, the electric field interacts with the interface throughout; this includes the region far from the contact lines. The electric field has the effect of pushing away the interface, thus decreasing the pressure of the droplet below the surrounding phase ($\Delta p < 0$). When the droplet turns into a film conformally adhering to the concave substrate, there is an additional contribution to the pressure, which pulls the interface back and opposes the electric stresses. Therefore, the decrease in electric field and the decrease in the pressure of the film thwart the spreading, and thus, a higher voltage V_T is required to achieve the same amount of spreading for a more concave surface.

We have, therefore, demonstrated how to produce thin, rectangular shaped, liquid films on the side of curved, flexible, liquid repellant substrates using dielectrophoresis forces. Furthermore, we have shown how the magnitude and sign of the curvature dependence of the film formation threshold voltage $V_T(\kappa_s)$ can be quantitatively reproduced from theoretical consideration of the balance of stresses acting on the films, including the Laplace pressure and the Maxwell stress. The physical insights from this work and the demonstration of programmable wettability on curved substrates provide the foundations for applications in, for example, imaging, electronic paper displays, and digital droplet microfluidic-based biochemical analysis devices with a range of variable curvatures, both positive and negative. Our work provides important insight into the curvature-dependent voltage driving conditions for dielectrophoresis driven liquid droplet actuation and transport by elucidating and quantifying the changes in switching behavior under substrate curvature. The versatility permitted by having flexible plastic substrates also offers the possibility of low-cost, and robust, disposable analytical flow devices. Furthermore, our work provides a basis for future exploration of thin liquid film creation on non-flat and flexible three-dimensional substrates with more complicated curvatures, including for the study of dynamic film dewetting mechanisms from complex morphologies.

See the supplementary material for details of our theoretical approach to modeling the electric potential of interdigitated electrodes in a cylindrical arrangement and, hence, to our derivation of the electric stresses on the liquid film, Eq. (2), calculated using the Maxwell stress tensor.

We gratefully acknowledge funding from the UK Engineering and Physical Sciences Research Council under Grant Nos. EP/R042276/1, EP/R036837/1, and EP/R036837/2. We gratefully acknowledge technical support from Russell Metcalfe and Ryan Toms at Nottingham Trent University.

AUTHOR DECLARATIONS

Conflict of Interest

The authors have no conflicts to disclose.

Author Contributions

E.R.-G. and P.J.B. contributed equally to this work. C.V.B., P.J.B., A.M.J.E., M.I.N., and I.C.S. conceived the research and designed the experiments. C.V.B., R.L.-A., M.I.N., and G.M. supervised the research. P.J.B. and A.M.J.E. performed the experiments. P.J.B., E.R.-G., and C.V.B. analyzed the results. E.R.-G., R.L.-A., and G.M. developed the theory. All authors discussed the ideas, results, and interpretation. C.V.B., E.R.-G., and P.J.B. wrote the manuscript with contributions from all authors.

DATA AVAILABILITY

The data that support the findings of this study are available from the corresponding author upon reasonable request.

REFERENCES

[1]G. Zhu, J. F. Yao, S. H. Wu, and X. D. Zhang, "Actuation of adaptive liquid microlens droplet in microfluidic devices: A review," Electrophoresis **40**(8), 1148 (2019).

[2]J. Li and C.-J. Kim, "Current commercialization status of electrowetting-on-dielectric (EWOD) digital microfluidics," Lab Chip **20**, 1705 (2020).

[3]A. M. J. Edwards, C. V. Brown, M. I. Newton, and G. McHale, "Dielectrowetting: The past, present and future," Curr. Opin. Colloid Interface Sci. **36**, 28 (2018).

[4]J. Barman, W. Shao, B. Tang, D. Yuan, J. Groenewold, and G. Zhou, "Wettability manipulation by interface-localized liquid dielectrophoresis: Fundamentals and applications," Micromachines **10**(5), 329 (2019).

[5]S. Xu, H. Ren, and S.-T. Wu, "Dielectro-phoretically tunable optofluidic devices," J. Phys. D **46**, 483001 (2013).

[6]X. Rui, S. Song, W. Wang, and J. Zhou, "Applications of electrowetting-on-dielectric (EWOD) technology for droplet digital PCR," Biomicrofluidics **14**(6), 061503 (2020).

[7]P. Teng, D. Tian, H. Fu, and S. Wang, "Recent progress of electrowetting for droplet manipulation: From wetting to superwetting systems," Mater. Chem. Front. **4**, 140 (2020).

[8]K. V. I. S. Kaler, R. Prakash, and D. Chugh, "Liquid dielectrophoresis and surface microfluidics," Biomicrofluidics **4**, 022805 (2010).

[9]D. Zhu, X. Zeng, C. Li, and H. Jiang, "Focus-tunable microlens arrays fabricated on spherical surfaces," J. Microelectricalmech. Syst. **20**(2), 389 (2011).

[10]Y.-S. Lu, H. Tu, Y. Xu, and H. Jiang, "Tunable dielectric liquid lens on flexible substrate," Appl. Phys. Lett. **103**, 261113 (2013).

[11]C. Li and H. Jiang, "Fabrication and characterization of flexible electrowetting on dielectrics (EWOD) microlens," Micromachines **5**, 432 (2014).

[12]K. L. Van Grinsven, A. O. Ashtiani, and H. Jiang, "Flexible electrowetting-on-dielectric microlens array sheet," Micromachines **10**(7), 464 (2019).

[13]S.-K. Fan, H. Yang, and W. Hsu, "Droplet-on-a-wristband: Chip-to-chip digital microfluidic interfaces between," Lab Chip **11**, 343 (2011).

[14]M. Abdelgawad, S. L. S. Freire, H. Yang, and A. R. Wheeler, "All-terrain droplet actuation," Lab Chip **8**, 672 (2008).

[15]D. Y. Kim and A. J. Steckl, "Electrowetting on paper for electronic paper display," Appl. Mater. Interfaces **2**(11), 3318 (2010).

[16]H. B. Eral, G. Manukyan, and J. M. Oh, "Wetting of a drop on a sphere," Langmuir **27**, 5340 (2011).

[17]Y. Wang and Y.-P. Zhao, "Electrowetting on curved surfaces," Soft Matter **8**, 2599 (2012).

[18]K. Xiao and C.-X. Wu, "Curvature effect of electrowetting-induced droplet detachment," J. Appl. Phys. **129**, 234701 (2021).

[19]R. Ahmed and T. B. Jones, "Dispensing picoliter droplets on substrates using dielectrophoresis," J. Electrost. **64**(7–9), 543 (2006).

[20]D. Chugh and K. V. I. S. Kaler, "Integrated liquid and droplet dielectrophoresis for biochemical assays," Microfluid. Nanofluid. **8**, 445 (2010).

[21]R. Prakash and K. V. I. S. Kaler, "Liquid dielectrophoresis dispensing of vesicles for on-chip nucleic acid isolation and detection," Colloids Surf., A **432**, 42 (2013).

[22]C. V. Brown, G. G. Wells, M. I. Newton, and G. McHale, "Voltage-programmable liquid optical interface," Nat. Photonics **3**, 403 (2009).

[23]G. McHale, C. V. Brown, M. I. Newton, G. G. Wells, and N. Sampara, "Dielectrowetting driven spreading of droplets," Phys. Rev. Lett. **107**, 186101 (2011).

[24]H. Geng, J. Feng, L. M. Stabrylac, and S. K. Cho, "Dielectrowetting manipulation for digital microfluidics: Creating, transporting, splitting, and merging of droplets," Lab Chip **17**, 1060 (2017).

[25]F. Mugele and J. Heikenfeld, *Electrowetting: Fundamental Principles and Practical Applications* (John Wiley & Sons, 2018).

[26]H. A. Pohl, *Dielectrophoresis the Behavior of Neutral Matter in Nonuniform Electric Fields*, Cambridge Monographs on Physics (Cambridge University Press, London, 1978).

[27]T. B. Jones, M. Gunji, M. Washizu, and M. J. Feldman, "Dielectrophoretic liquid actuation and nanodroplet formation," J. Appl. Phys. **89**(2), 1441 (2001).

[28]J. D. Jackson, *Classical Electrodynamics* (John Wiley & Sons, Inc., 1999).

[29]P.-G. de Gennes, F. Brochard-Wyart, and D. Quere, *Capillarity and Wetting Phenomena Drops, Bubbles, Pearls, Waves* (Springer, 2004).

[30]C. V. Brown, G. McHale, and N. J. Mottram, "Analysis of a static undulation on the surface of a thin dielectric liquid layer formed by dielectrophoresis forces," J. Appl. Phys. **110**, 024107 (2011).